Celal Bayar University Journal of Science

Thermal Performance Analysis of a Liquid Cooling Plate for Power Electronics

Mehmet Bahattin AKGÜL[1]*, Furkan Sinan ERÇEL[2]

[1] Department of Mechanical Engineering, Manisa Celal Bayar University, 45140 Muradiye, Manisa, Turkiye
[2] R&D Department, Coşkunöz Kalıp Makine, 16000 Nilüfer, Bursa, Turkiye
* mbakgul@gmail.com
* Orcid No: 0000-0002-8916-1171

Received: 6 August 2024
Accepted: 16 September 2024
DOI: 10.18466/cbayarfbe.1528939

Abstract

The need for effective cooling methods has become very critical because of the miniaturization and increasing heat flux density in power electronics equipment. The power electronics systems must have good thermal management engineering for efficiency and safe operation. Due to increasing heat loads, liquid cooling options are more preferred than the air cooling solutions. In this study, thermal performance of a liquid cooling plate is investigated by using computational fluid dynamics (CFD) tools. Different flow path configurations are examined for homogeneous and effective cooling of power electronics equipments with high power density. The pressure losses, surface temperatures and thermal resistances at different coolant flow rates are computed and compared together. Moreover, the influence of the cooling channel height and width on the thermal thermal performance is analyzed.

Keywords: Liquid Cooling, Cold Plate, CFD, IGBTs

1. Introduction

The insulated-gate bipolar transistors (IGBTs) are widely used as voltage-controlled switching element in power electronic applications. IGBTs can dissipate significant amount of heat during operation despite their small size. The junction temperatures of IGBTs must be kept at certain levels for operating safely at high performance. Taking into consideration the criteria such as size and weight, liquid cooling of IGBTs modules is more preferred than air cooled systems. IGBTs are generally mounted on a cold plate and junction temperatures are kept at the desired values by means of coolant circulation in liquid cooling applications. The cold plate studies which provide homogeneous cooling at low pressure losses have been the subject of many studies in the literature [1-18]. İlikan and Yayli [19] numerically investigated performances of three liquid cold plates with different flow configurations for li-ion battery cells in electric vehicle applications. Hetsroni et al. [20] studied the steady-state heat transfer for different types of microchannels for electronics cooling. They obtained a significant enhancement of heat transfer under the conditions of flow boiling in microchannels. Özbektaş et al. [21] numerically investigated the effect of flow circulation pattern and velocity on the performance of water-cooled heat sink. They showed that pressure difference, outlet temperature, power consumption, and heat transfer rate to air increased by increasing Reynolds number. Jayarajan and Azimov [22] proposed a novel cold plate design featuring a zig-zag serpentine flow pattern within a rectangular profile channel. Their study found that the increases in mass flow rate reduced the maximum temperature, and improved surface standard temperature and heat transfer rate but increases the pressure drop by nearly 49% Akbarzadeh et al. [23] conducted a new cold plate study for liquid cooling of lithium-ion batteries. They reduced the pump power by 30% and achieved more homogeneous cooling with their newly developed cold plate. Huo et al. [24] designed a mini-channel cold plate for prismatic battery cells. They examined the effects of coolant flow rate, flow direction and ambient temperature in their studies. Jin et al. [25] developed a new cold plate with an oblique fin structure. They indicated that oblique finned cold plates were able to maintain the average temperature of the battery surface below 50 °C for a heat load of 1240 W at a flow rate of less than 0.9 l/min. Jassem and Salem [26] carried out experimental and numerical investigations of a finned cold plate under different conditions. They significantly increased the cold plate performance in their study. Pan

et al. [27] examined the performance of IGBT modules by way of integrating a vapor chamber into the cold plate utilized for cooling. They indicated that the performance of the cold plate integrated with the vapor chamber improved. Reeves et al. [28] examined the cooling performance by adding a novel fin pattern to the cold plate utilized in power electronics applications. They indicated that novel fin structure improved heat transfer without significant pressure loss. Zhang et al. [29] investigated cold plates with linear, S and helix type flow configurations for cooling IGBT modules. They found that the cold plate of S-type with guide plates possess the favorable thermal performance. Zhang et al. [30] carried out CFD investigation of two novel designs of variable cross-section overflow channels of manifold cold plates for lithium-ion batteries. They reported that the average temperature of the cooling plate surface of the novel manifold design decreased by 3.65 K compared to the conventional manifold unit. Chu et al. [31] found that the heat transfer coefficient of hybrid nanofluid drastically enhances compared to distilled water for varying the inlet velocity. Nada et al. [32] reported that the nanofluid provides an enhancement of the heat transfer rate compared to water due to the higher thermal conductivity of the nanoparticles.

In this study, the performance analysis of a cold plate integrated with two IGBT modules used in power electronics applications is carried out for different flow configurations and coolant flow rates. The cooling performance is investigated for series, parallel and series-parallel flow configurations. The temperature distributions and thermal resistances of the cold plate with pressure losses are determined at different flow rates and presented graphically. The effects of the cooling channel height and width on the thermal performance are examined. The proposed series-parallel flow configuration contributes to the effective cooling of IGBTs modules.

2. Methodologies

2.1. Physical Model of Cold Plate

Fig.1 (a) shows IGBTs mounted cold plate. The cold plate consists of a main metal block, cover and coolant inlet/outlet adapters as given in Fig.1 (b). Generally, high thermal conductivity metals such as aluminum are used for producing cold plates. In this study, main metal block material is chosen AL 6063 alloy and cover is Al 1050. Two PrimePack3 IGBT modules are mounted on the cold plate. The modules are cooled by coolant which circulates within the machined flow channels inside the main block. A mixture of 50% ethylene glycol in 50% water is used as the coolant. The thermophysical properties of the coolant and solid materials are given in Table 1.

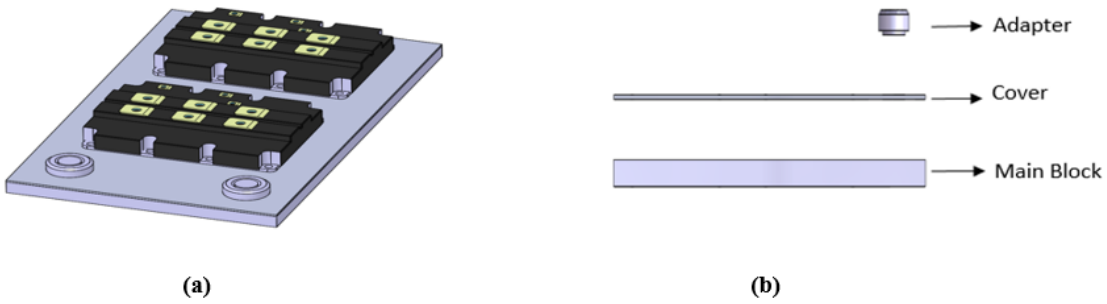

Figure 1. (a) IGBT mounted cold plate; (b) Assembly of subcomponents of the cold plate.

Table 1. Material Properties

Material	Density ($kg \cdot m^{-3}$)	Specific Heat (J/(kgK))	Dynamic Viscosity (Pa.s)	Thermal Conductivity (W/mK)
Al 1050	2705	900	-	227
Al 6063	2700	900	-	200
Coolant	1045	3425	0.002	0.41

Three flow configurations are considered in order to examine thermal performance of cold plate. Coolant flow paths such as serial, parallel and serial/parallel are machined inside the cold plate and shown in Fig.2. Cross-sectional dimensions of the flow channels are the same for all configurations.

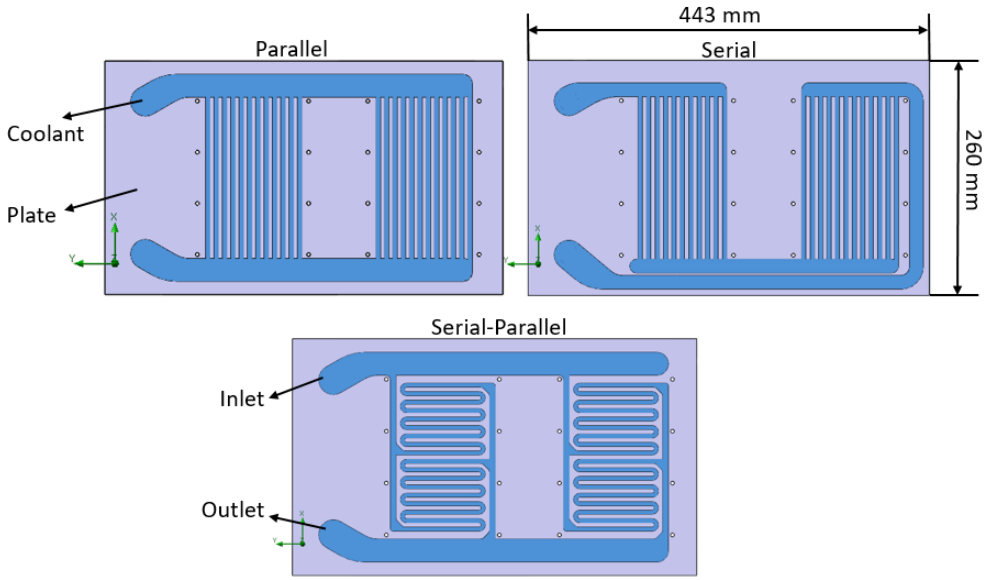

Figure 2. Flow configurations of the cold plate

2.2. Numerical Model and Grid Dependence Verification

The Simcenter FLOEFD [33] is used to perform numerical analysis and this commercial software is based on a 3D finite volume solver for the Navier-Stokes and energy equations. The computational domain consists of solid and fluid regions. Solid regions represent the cold plate body and fluid regions indicate the coolant. Incompressible flow and steady state conditions are assumed for the analysis. The governing equations are expressed as follows:

Continuity equation:

$$\nabla.\vec{V} = 0 \tag{1}$$

Momentum equation:

$$\rho(\vec{V}.\nabla\vec{V}) = -\nabla p + \mu\cdot\nabla^2\vec{V} \tag{2}$$

Energy equations for fluid and solid domains are respectively given as:

$$\rho c_p(\vec{V}.\nabla T) = k_f\nabla^2 T \tag{3}$$

$$k_s\nabla^2 T = 0 \tag{4}$$

In these equations, , ρ is the coolant density, μ, k and c_p are the dynamic viscosity, thermal conductivity and specific heat, respectively. P is the pressure, V is the mean velocity vector and T is the temperature.

The coolant inlet temperature of 55 °C is used for all the simulations. Flow rates are defined as 10, 15 and 20 l/min, respectively. The standard k-ε turbulent model is used to model turbulent flow. Pressure at the cold plate outlet is set to 100 kPa. In the analysis, each IGBTs module is assumed to dissipate heat a rate of 2 kW. The effective heat dissipation region of IGBT elements is generally in the middle region, which comprises about 50% of the contact surface. The constant heat flux is applied to the 50% of the IGBTs total contact area. The other surfaces of the cold plate is considered as adiabatic. The schematic presentation of the boundary conditions is given in Fig.3 and summarized in Table 2.

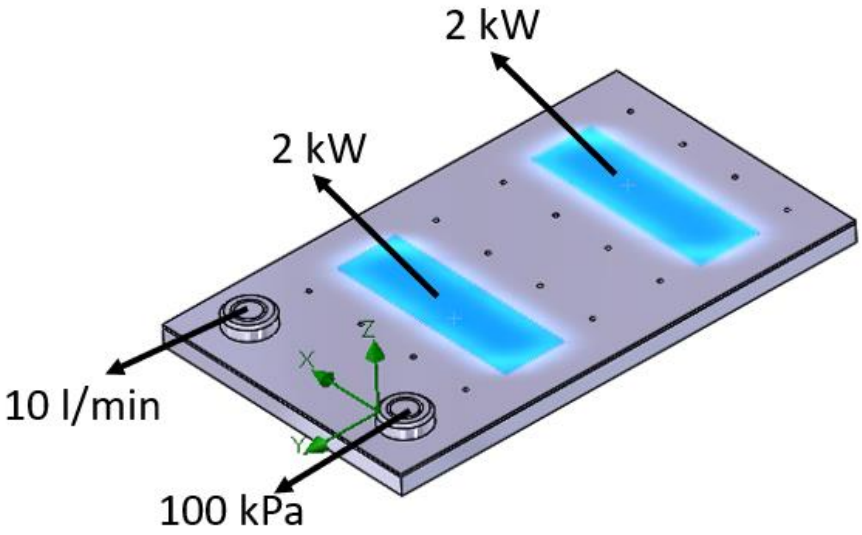

Figure 3. Boundary conditions

Table 2. Details of the boundary conditions

Inlet	Volume flow inlet
Outlet	Pressure outlet
Fluid-solid interface surface	Coupled wall
IGBTs mounting surfaces	Constant heat flux
Other surface	Adiabatic

In order to evaluate thermal performance of the cold plate, some performance parameters need to be defined. Maximum surface temperature ($T_{s,max}$), pressure drop of the coolant (ΔP) across the cold plate, thermal resistance (R_{th}) and the effectiveness (ε) of the cold plate are considered as main parameters. Thermal resistance and effectiveness equations are given as follows:

$$R_{th} = \frac{T_{s,\max} - T_{c,in}}{Q}, \quad (\frac{^0C}{kW}) \tag{5}$$

$$\varepsilon = \frac{T_{c,o} - T_{c,in}}{T_{s,\max} - T_{c,in}} \tag{6}$$

where $T_{s,max}$ is the maximum surface temperature of the cold plate, Q is the total heat load of the IGBTs, $T_{c,in}$ and $T_{c,o}$ are the coolant inlet and outlet temperatures, respectively.

A grid is created by the hexahedral elements in the computational domain. High-resolution mesh is adopted in the vicinity of the boundary layer region for the simulation accuracy. Fig. 4 presents the created grid structure. The total number of grids of 0.7, 1.1, 1.3 and 1.75 million are applied for the grid dependence test in the computational domain. The purpose of the grid dependence study is to obtain precision solution with smaller number of elements. The results of the grid dependence study are given in Fig. 5. The results of the surface temperature and pressure drop indicate about 0.1% variation for more than 1.39 million grid elements.

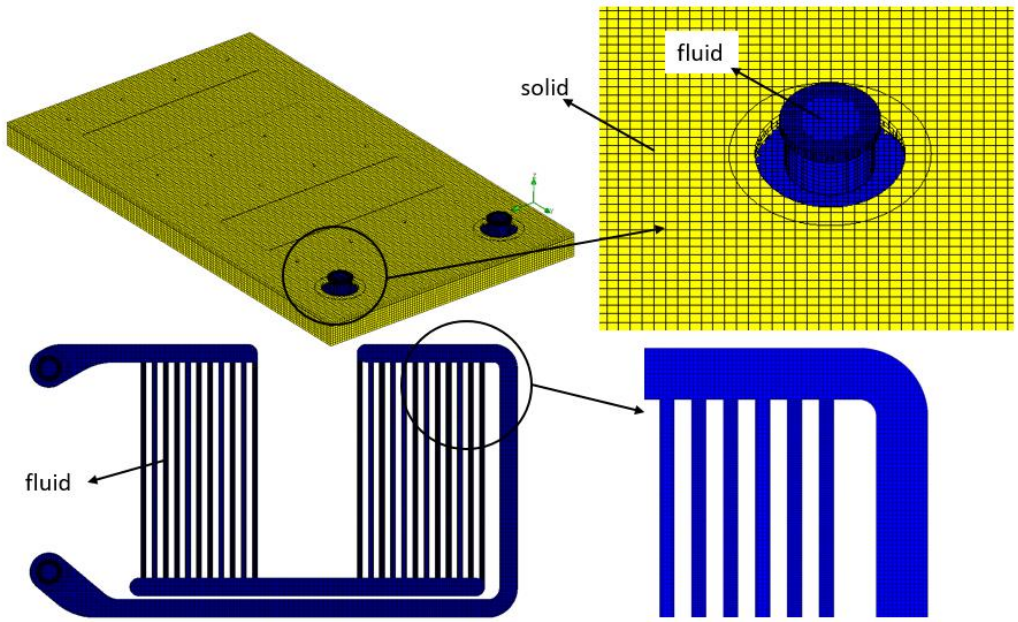

Figure 4. Grid structure

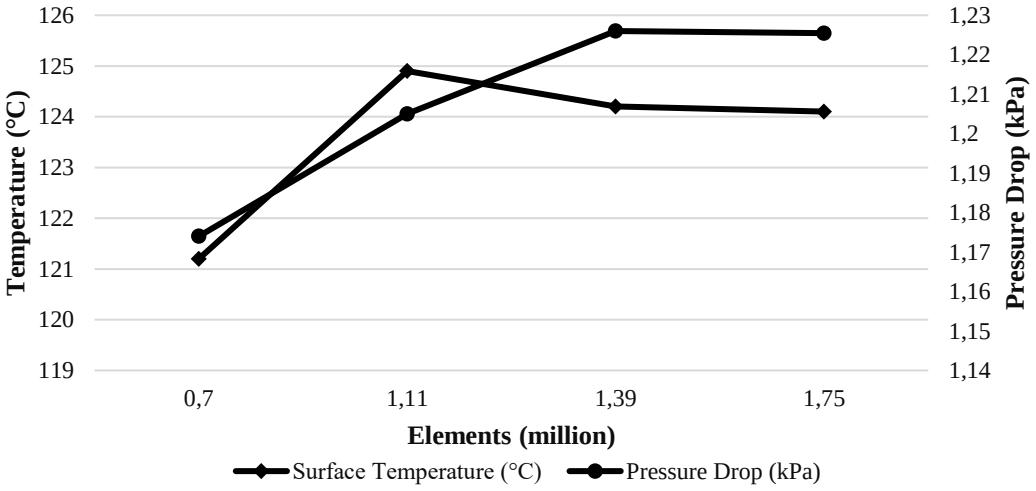

Figure 5. Effects of grid number on the pressure drop and surface temperature.

3. Results and Discussion

3.1. Effects of Flow Channel Configuration

The thermal analysis of a cold plate with three different flow channel structure is conducted for various flow rates. The velocity, pressure and temperature distributions are compared for the three flow channel configuration. Surface temperatures of the cold plate are given in Fig. 6 for different flow rates. The lowest surface temperature is observed on the serial-parallel channel configuration. In addition to this, the maximum surface temperature of the parallel channel is higher than that of serial. Also, it is observed that the temperature distribution in the serial-parallel channel configuration is more homogeneous on the IGBTs mounting surfaces

compared with the other configurations. It is apparent that as the flow rate increases, the maximum and average surface temperatures of the cold plate decreases due to strong convection effects.

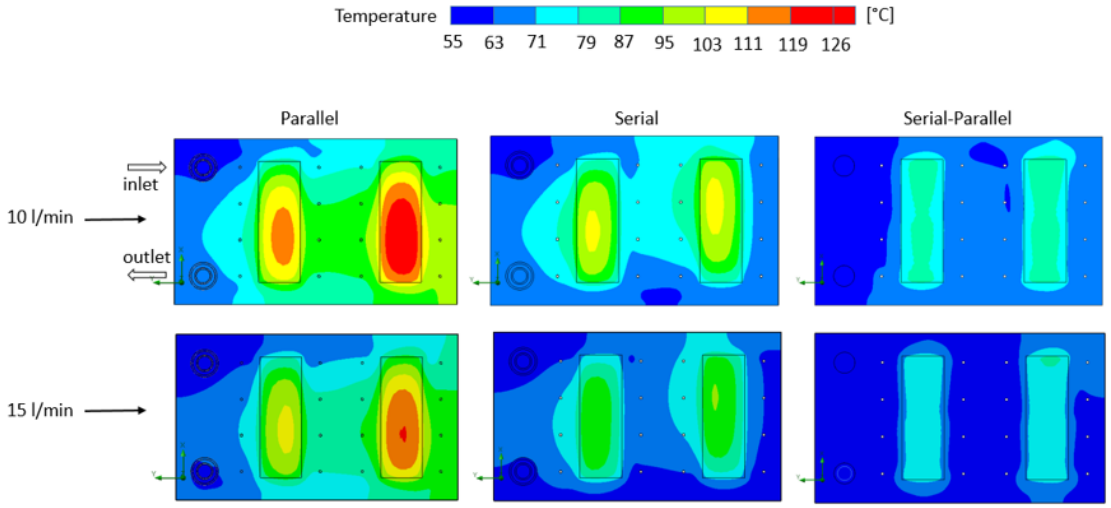

Figure 6. Temperature distribution on the cold plate for different flow rates

Table 3. Effectiveness and thermal resistance values of cold plate for flow rate of 10 l/min

Channel Type	ε	R_{th}
Parallel Channel	0.0968	17.3
Serial Channel	0.1233	12.15
Serial-Parallel Channel	0.2272	7.33

The computed thermal resistance and effectiveness values are presented in Table 3 for flow rate of 10 l/min. The low thermal resistance implies that the plate transfers the more heat from the IGBT module. To make a comparison of the thermal resistances, the lowest thermal resistance occurs in the series-parallel channel, while the highest thermal resistance occurs in the parallel channel cooling plate. On the contrary of the thermal resistance, effectiveness value is the highest for the case of serial-parallel configuration. This is because decrease in the maximum surface temperature and improved the temperature uniformity.

Fig. 7 shows the velocity distributions in the mid-height plane for different flow rates. It can be seen that, the velocity of the coolant in the parallel channels is significantly slower than other configurations. The low flow velocity values cause high surface temperature and poor temperature uniformity on the cold plate surface. A more uniform velocity distribution is achieved in the serial-parallel configuration compared to the serial flow channels. In addition to this, the flow velocity values increase by the flow rate.

Celal Bayar University Journal of Science
Volume 20, Issue 4, 2024, p 72-81
Doi: 10.18466/cbayarfbe.1528939

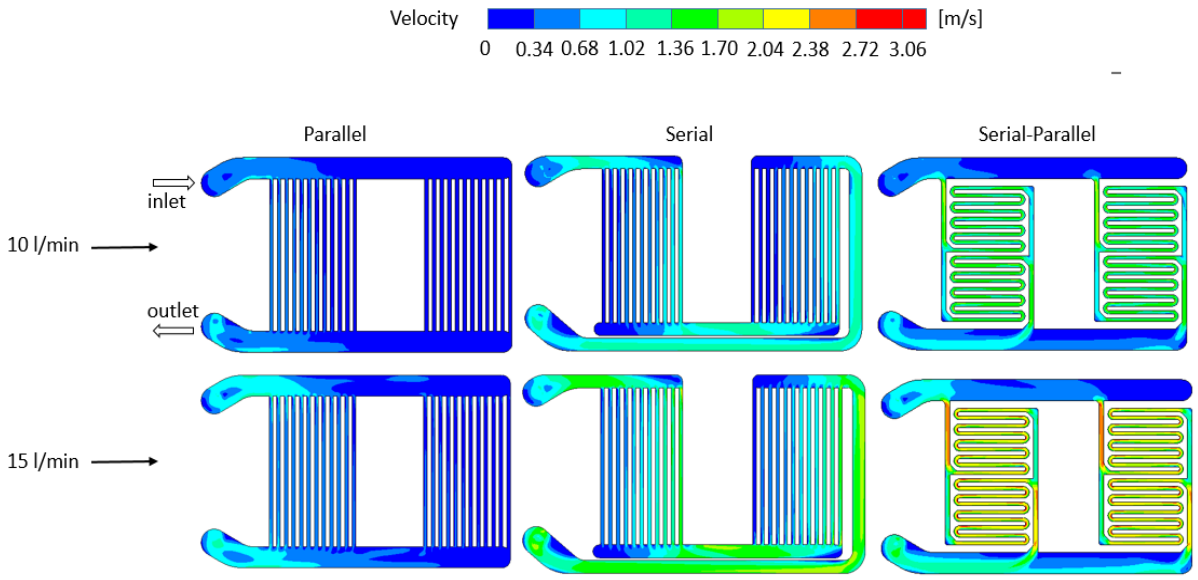

Figure 7. Velocity distribution on the cold plate for different flow rates

The thermal resistance and pressure drop values are presented in Fig. 8 and 9 for various flow rates. The cooling performance of the cold plate is significantly enhanced for serial-parallel flow configuration for each flow rate. The thermal resistance decreases for all flow configurations with the increase of flow rate due to strengthening of convection effects. Pressure drop values increase with the increase of the flow rate. This increase is much more evident for the case of serial-parallel flow configuration due to high coolant velocity in the flow channels and extra minor losses arising from the channel structure.

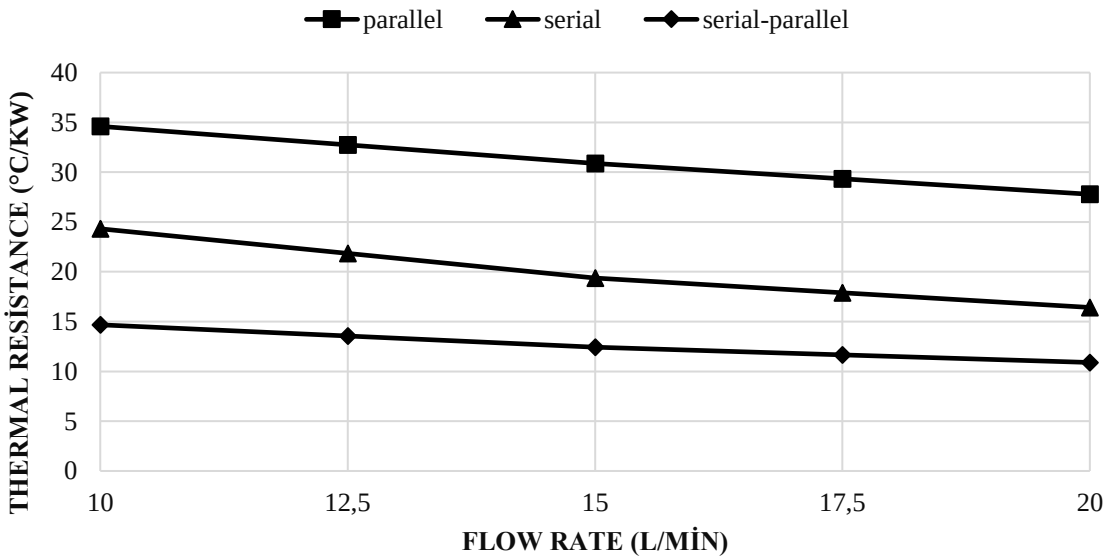

Figure 8. Variation of thermal resistance for different flow rate values

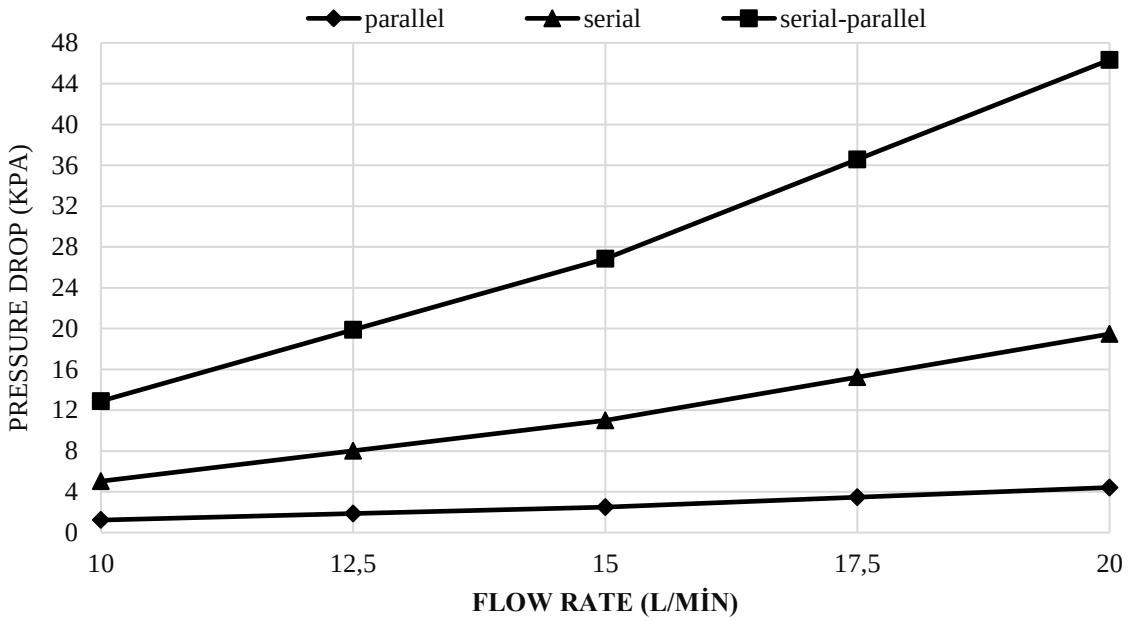

Figure 9. Variation of pressure drop for different flow rate values

3.2. Effects of Channel Aspect Ratio

The flow channel dimensions play a vital role for effective heat removal with optimum pumping power for the cold plate applications. The presentation of the flow channels is given in Fig. 10. The effect of the aspect ratio (defined as the ratio of channel height to the channel width) on the cooling performance is analyzed in this section for the serial-parallel configuration.

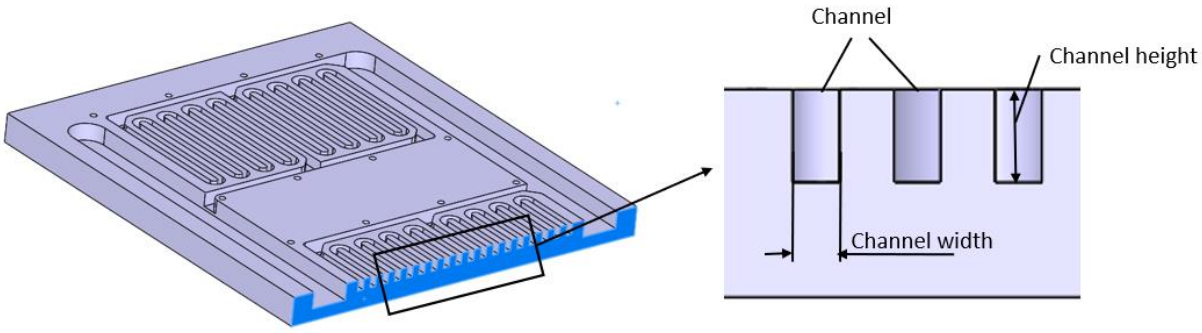

Figure 10. Schematic diagram of channel layout

The surface temperature distribution of the cold plate for flow rate of 10 l/min is shown in Fig. 11. It is obvious that the surface temperature of the cold plate with aspect ratio of 1.1 is lesser than other two cases. For fixed flow rate, the coolant velocity increases with the decrease of the aspect ratio. Larger coolant velocities indicate more powerful convective heat transfer. As shown in Table 4, the aspect ratio plays dominant role in the cold plate pressure drop. The pressure drop increases about two-fold when the aspect ratio decreases to 1.1 from 1.7. Also, it is observed that the effect of the aspect ratio on the thermal resistance is lower compared to the pressure drop.

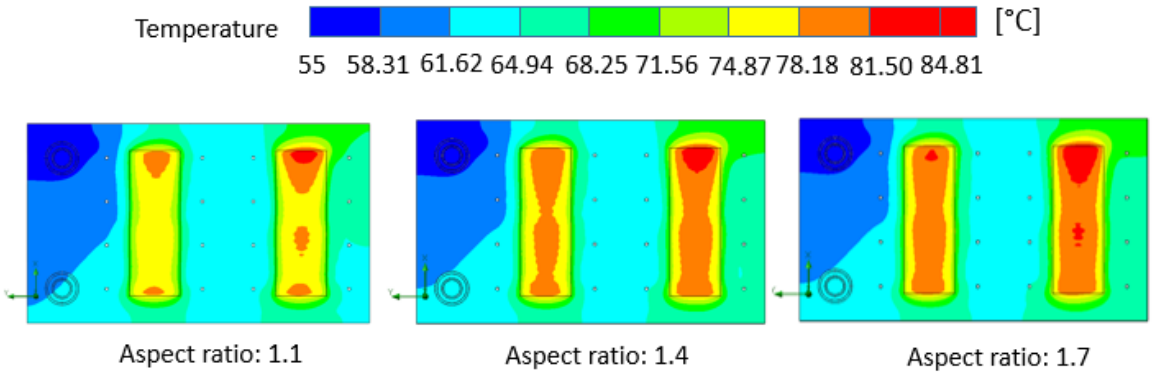

Figure 11. Surface temperature distributions for various aspect ratios

Table 4. Thermal resistance, pressure drop and maximum surface temperature values for various aspect ratios

Aspect Ratio	1.1	1.4	1.7
R_{th} (^{0}C/kW)	7.10	7.33	7.47
ΔP (kPa)	19.69	12.83	10.13
T_{max} (^{0} C)	83.41	84.35	84.88

4. Conclusion

In this study, the performance analysis of a cold plate containing two IGBTs utilized in the rail system applications is carried out for different flow configurations and coolant flow rates. Three different flow configurations are studied namely series, parallel and series-parallel. Temperature distributions, thermal resistance and pressure drops in the cold plate for different flow rates are obtained by using commercial software. According to the analysis results, the maximum temperature decreases significantly for series-parallel flow configuration. The thermal resistance decreases about 60% in the case of serial-parallel configuration comparing with the parallel flow channels. Moreover, despite the improvement in the thermal resistance, pressure drop values for serial parallel configuration are a 10 times higher than in parallel configuration. In addition to this with the increase of the channel aspect ratio, pressure drop decreases by 48.5% while the thermal resistance increases by only %5. The serial-parallel channel configuration can provide a significant performance improvement in electronic cooling applications with proper aspect ratio optimization.

Author's Contributions

Mehmet Bahattin Akgül: Drafted and wrote the manuscript, performed the analytical analysis and result.

Furkan Sinan Erçel: Assisted in analytical analysis on the structure, supervised the experiment's progress, result interpretation and helped in manuscript preparation.

Ethics

There are no ethical issues after the publication of this manuscript.

References

[1]. Kandlikar, S.G. and Hayner, C.N. 2009. Liquid cooled cold plates for industrial high-power electronic devices thermal design and manufacturing considerations. Heat Transfer Engineering; 30(12), 918–930.

[2]. Teng H., Yeow, K. 2012. Design of direct and indirect liquid cooling systems for high- capacity, high-power lithium-ion battery packs. SAE International Journal of Alternative Powertrains; 1(2), 525-536.

[3]. Jarrett A, Kim IY. 2011. Design optimization of electric vehicle battery cooling plates for thermal performance. Journal of Power Sources; 196(23):10359–68

[4]. Maddipati, U. R., Rajendran, P., & Laxminarayana, P. 2013. Thermal design and analysis of cold plate with various proportions of ethyl glycol water solutions. International Journal of Advanced Trends in Computer Science and Engineering; 2(6), 22-25.

[5]. Lu, Z., Zhang, K. 2021. Study on the performance of a Y-shaped liquid cooling heat sink based on constructal law for electronic chip cooling. Journal of Thermal Science and Engineering Applications; 13(3), 034501.

[6]. Datta, A.B., Majumdar, A.K. 1980. Flow distribution in parallel and reverse flow manifolds, International Journal of Heat and Fluid Flow; 2(4), 253-262

[7]. Chen, D., Jiang J., Kim, G., Yang, C., Pesaran, A. 2016. Comparison of different cooling methods for lithium ion battery cells, Applied Thermal Engineering; 94(1), 846-854.

[8]. Panchal, S., Mathewson, S., Fraser, R., Culham, R., Fowler, M. 2015. Thermal management of lithium-ion pouch cell with indirect liquid cooling using dual cold plates approach, SAE International Journal of Alternative Powertrains; 4(2), 293-307.

[9]. Teng, H., Ma, Y., Yeow, K., Thelliez, M. 2011. Thermal characterization of a li-ion battery module cooled through aluminum heat-sink plates, SAE International Journal of Passenger Cars—Mechanical Systems; 4(3), 1331-1342.

[10]. Yeow, K., Teng, H., Thelliez, M., Tan, E. 2012. Thermal analysis of a li-ion battery system with indirect liquid cooling using finite element analysis approach, SAE International Journal of Alternative Powertrains; 1(1), 65-78.

[11]. Yeow, K., Teng, H. 2013. Reducing temperature gradients in high-power, large-capacity lithium-ion cells through ultra-high thermal conductivity heat spreaders embedded in cooling plates for battery systems with indirect liquid cooling, SAE World Congress & Exhibition; Detroit, USA, 1(0234), 1-11.

[12]. Ming-Chang, L., Chi-Chuan, W. 2006. Effect of the inlet location on the performance of parallel-channel cold-plate, IEEE Transactions on Components and Packaging Technologies; 29 ,30–38.

[13]. Hetsroni G., Mosyak A., Segal Z. 2001. Nonuniform temperature distribution in electronic devices cooled by flow in parallel microchannels, IEEE Transactions on Components and Packaging Technologies; 24, 16–22.

[14]. Muratçobanoğlu, B., Mandev, E., Ceviz, M. A., Manay, E., & Afshari, F. 2024. CFD simulation and experimental analysis of cooling performance for thermoelectric cooler with liquid cooling heat sink. Journal of Thermal Analysis and Calorimetry; 149(1), 359-377.

[15]. Zhang, F., Huang, Z., Li, S., Sun, S., & Zhao, H. 2024. Design and thermal performance analysis of a new micro-fin liquid cooling plate based on liquid cooling channel finning and bionic limulus-like fins. Applied Thermal Engineering; 237, 121597.

[16]. Chu, Y. M., Farooq, U., Mishra, N. K., Ahmad, Z., Zulfiqar, F., Yasmin, S., & Khan, S. A. 2023. CFD analysis of hybrid nanofluid-based microchannel heat sink for electronic chips cooling: applications in nano-energy thermal devices. Case Studies in Thermal Engineering; 44, 102818.

[17]. Li, W., Garg, A., Wang, N., Gao, L., Le Phung, M. L., & Tran, V. M. 2022. Computational fluid dynamics-based numerical analysis for studying the effect of mini-channel cooling plate, flow characteristics, and battery arrangement for cylindrical lithium-ion battery pack. Journal of Electrochemical Energy Conversion and Storage; 19(4), 041003.

[18]. Zhang, F., Tao, Y., He, Y., & Qiu, S. 2024. Optimization and thermal characterization of a new liquid-cooled plate with branching channels of fractal geometry. Applied Thermal Engineering; 123881.

[19]. İlikan A. N., Yaylı, A. 2022. Performance comparison of parallel and series channel cold plates used in electric vehicles by means of CFD simulations. Eskişehir Osmangazi Üniversitesi Mühendislik ve Mimarlık Fakültesi Dergisi; 30(3), 397-404.

[20]. Jafarı, R. 2021. Dimensional optimization of two-phase flow boiling in microchannel heat sinks. International Advanced Researches and Engineering Journal; 5(3), 475-483.

[21]. Özbektaş S., Sungur B., and Topaloğlu B. 2022. Numerical investigation of the effect of flow circulation pattern and velocity on the performance of water-cooled heat sink. Gümüşhane Üniversitesi Fen Bilimleri Dergisi; 12(1), 151-163.

[22]. Jayarajan, S. A., & Azimov, U. 2023. CFD Modeling and Thermal Analysis of a Cold Plate Design with a Zig-Zag Serpentine Flow Pattern for Li-Ion Batteries. Energies; 16(14), 5243.

[23]. Akbarzadeh, M., Jaguemont, J., Kalogiannis, T., Karimi, D., He, J., Jin, L., et al., 2021. A novel liquid cooling plate concept for thermal management of lithium-ion batteries in electric vehicles. Energy Conversion. Management; 231, 113862.

[**24].** Huo Y, Rao Z, Liu X, Zhao J. 2015. Investigation of power battery thermal management by using mini-channel cold plate. Energy Conversion Management; 89:387–95.

[25]. Jin LW, Lee PS, Kong XX, Fan Y, Chou SK. 2014. Ultra-thin minichannel LCP for EV battery thermal management. Applied Energy; 113:1786–94.

[26]. Jassem, R. R., & Salem, T. K. 2016. An experimental and Numerical study the performance of finned Liquid cold-plate with different operating conditions. International Journal of Current Research and Review; 9(3), 41-46.

[27]. Pan, M. 2021. Study of the performance of an integrated liquid cooling heat sink for high-power IGBTs. Applied Thermal Engineering; 190, 116827..

[28]. Reeves, M., Moreno, J., Beucher, P., Loong, S. J., & Brown, D. 2011. Investigation on the impact on thermal performances of new pin and fin geometries applied to liquid cooling of power electronics. In PCIM Europe ; 772-778.

[29]. Zhang, Y. P., Yu, X. L., Feng, Q. K., & Zhang, R. T. 2009. Thermal performance study of integrated cold plate with power module. Applied Thermal Engineering; 29(17-18), 3568-3573.

[30]. Zhang, H., Ganesan, P., Sharma, R. K., Zubir, M. N. B. M., Badruddin, I. A., & Chong, W. T. 2024. A novel overflow channel design of manifold cold plate for lithium-ion battery: A CFD study. Process Safety and Environmental Protection; 189, 648-663.

[31]. Chu, Y. M., Farooq, U., Mishra, N. K., Ahmad, Z., Zulfiqar, F., Yasmin, S., & Khan, S. A. 2023. CFD analysis of hybrid nanofluid-based microchannel heat sink for electronic chips cooling: applications in nano-energy thermal devices. Case Studies in Thermal Engineering; 44, 102818.

[32]. Nada, S. A., El-Zoheiry, R. M., Elsharnoby, M., & Osman, O. S. 2022. Enhancing the thermal performance of different flow configuration minichannel heat sink using Al2O3 and CuO-water nanofluids for electronic cooling: An experimental assessment. International Journal of Thermal Sciences; 181, 107767.

[33]. User manual of software FloEFD.